

Article

Fluid–Solid Coupling Model and Simulation of Gas-Bearing Coal for Energy Security and Sustainability

Shixiong Hu ¹, Xiao Liu ^{1,2,*} and Xianzhong Li ^{1,2}

¹ School of Energy Science and Engineering, Henan Polytechnic University, Jiaozuo 454003, China; 211702020003@home.hpu.edu.cn (S.H.); lixianzhong@hpu.edu.cn (X.L.)

² Collaborative Innovation Center of Methane (Shale Gas) in Central Plains Economic Zone, Jiaozuo 454003, China

* Correspondence: liuxiao@hpu.edu.cn;

Received: 10 January 2020; Accepted: 19 February 2020; Published: 24 February 2020



Abstract: The optimum design of gas drainage boreholes is crucial for energy security and sustainability in coal mining. Therefore, the construction of fluid–solid coupling models and numerical simulation analyses are key problems for gas drainage boreholes. This work is based on the basic theory of fluid–solid coupling, the correlation definition between coal porosity and permeability, and previous studies on the influence of adsorption expansion, change in pore free gas pressure, and the Klinkenberg effect on gas flow in coal. A mathematical model of the dynamic evolution of coal permeability and porosity is derived. A fluid–solid coupling model of gas-bearing coal and the related partial differential equation for gas migration in coal are established. Combined with an example of the measurement of the drilling radius of the bedding layer in a coal mine, a coupled numerical solution under negative pressure extraction conditions is derived by using COMSOL Multiphysics simulation software. Numerical simulation results show that the solution can effectively guide gas extraction and discharge during mining. This study provides theoretical and methodological guidance for energy security and coal mining sustainability.

Keywords: fluid–solid coupling; coal containing gas; permeability; energy safety; sustainability

1. Introduction

Since the 21st century, global resource shortage and environmental pollution have become difficult problems in human sustainability development [1,2]. Policy makers in various countries have focused on sustainable energy and low-carbon development by proposing sustainable strategies and methods [3]. With the advent of low-carbon economy, coalbed methane, as a clean, efficient, and safe energy source, has been eliciting considerable research attention. This unconventional natural gas is mainly present in coal seams in free and adsorption states [4]. Coal is a typical dual-porosity/permeability system containing a porous matrix surrounded by fractures. The coal matrix is separated by a natural fracture network composed of butt cleats and face cleats. The cleat system provides an effective flow channel for gas. The developed pore structure is the main space for coalbed methane. During gas percolation of porous media, the effective stress of the porous medium skeleton changes because of the change in pore pressure; the porosity and permeability of porous media also change to a certain extent [5]. These changes can affect the gas flow in pores and the redistribution of gas pressure within a certain range. Therefore, in studying the migration rule and deformation characteristics of gas in a porous medium, such as coal, the interaction between the gas flow in a porous medium and the deformation of the porous medium body should be considered. The mutual coupling between the gas seepage flow field and the stress field in the porous medium should also be considered.

Through relevant laboratory tests and field practice, people have gradually realized that the seepage property of gas in coal is related to the mechanical properties of coal, gas pressure, in situ stress, temperature, and other factors. Sommerton et al. studied the effect of stress on the gas seepage property of coal [6]. Brace investigated the law of permeability change of rock mass under stress [7]. McKee et al. analyzed the relationship between stress and coal porosity and permeability and studied the phenomenon in which the depth of coal seams and effective stress increase, the width of cleats in coal seam decreases, and permeability decreases exponentially [8]. Enever et al. obtained the influence rule between the effective stress and permeability of coal [9]. In accordance with the generalized form of the power law, Sun established a mathematical model for the flow of compressible gas in coal seams. This model, which is called the nonlinear gas flow model, was based on the measured gas parameters in the Zhongmacun Coal Mine of Jiaozuo Mining Bureau. A numerical simulation of the pressure distribution of the homogeneous gas seepage flow field was carried out using various models [10–12]. Li et al. studied the relationship among coal adsorption expansion, deformation, porosity, and permeability in consideration of the adsorption deformation characteristics of the coal skeleton and obtained the relationship among porosity, permeability, and swelling deformation [13,14]. Tao et al. analyzed the problems existing in the theory of nonlinear gas flow and theory of fluid–solid coupling of coal-bed gas. The research achievements in the fields of nonlinear gas flow theory, gas flow theory of the geothermal field effect, and coal-bed gas fluid–solid coupling theory have been scrutinized extensively [15,16]. Zhu et al. considered the Klinkenberg effect and proposed a coupled mathematical model of solid deformation and gas flow [17–20].

However, the fluid–solid coupling model that scholars have established still has certain limitations. For example, the Klinkenberg and adsorption expansion effects on gas migration in coal were not considered simultaneously. Existing research shows that strain on adsorption expansion occurs after the coal body adsorbs gas. When the strain is limited by certain factors, adsorption expansion stress follows, which causes a certain degree of primary deformation of the coal skeleton and affects the development of coal pores. Thus, the effect of adsorption expansion on gas migration should not be ignored [21]. On the basis of previous studies, the author comprehensively considers the influence of the two factors of migration of coalbed methane in coal and establishes a mathematical model of fluid–solid coupling in a low-permeability coal seam. Thereafter, relevant partial differential equations are derived. The establishment of the model expands the theory of fluid–solid coupling of gas-bearing coals under multi-field conditions and clarifies the law of gas occurrence and seepage in coal. The establishment of the fluid–solid coupling equation can characterize gas flow in coal seams from the perspective of time and improve the research method of gas dynamic flow law. The rationality of the established mathematical model is verified by using a specific example of the effective extraction radius of coal mine gas. This model provides a theoretical basis for the design and layout of gas drainage boreholes in coal mining and a reasonable reference for decision makers to control coal mine gas effectively [22,23].

2. Mathematical Model

2.1. Basic Assumptions

- (1) Coal containing gas can be regarded as an isotropic elastic medium.
- (2) The coal seam is considered homogeneous, that is, the physical properties of each part of the coal seam are similar everywhere and do not change with a change in position.
- (3) The coal seam temperature is constant.
- (4) The gas contained in the coal seam is regarded as ideal gas and obeys the ideal gas state equation. The gas desorption obeys the Langmuir equation.
- (5) The seepage characteristic of coalbed methane in coal meets the Klinkenberg effect.
- (6) The deformation of coal is small.
- (7) The overall deformation of coal rock consists of pore and fracture deformation.

- (8) Single-phase saturated gas fluid exists in the coal seam, and only free and adsorbed states are available.
- (9) The model is isolated from the outside world and does not undergo any form of energy and material exchange.

2.2. Physical Property Parameter Model of Coal

The compression and adsorption expansion of deformation result in different degrees of deformation of the coal skeleton because of the changes in conditions of the coal seam, such as crustal stress and gas pressure. Owing to the different depths of the coal seam, the gas pressure and crustal stress also change to varying degrees, resulting in changes in coal seam porosity and permeability.

2.2.1. Deformation Mechanism of Coal Containing Gas

According to previous research results [24], two kinds of deformation mechanisms exist under the joint action of internal and external stresses of coal containing gas.

- (1) Structural deformation: Relative dislocation occurs between coal particles because of external stress. The particle arrangement becomes increasingly compact, which causes the compression of the coal particle skeleton. The deformation caused by the two is called structural deformation, as shown in Figure 1.
- (2) Body deformation: The deformation of coal particles is mainly caused by the adsorption expansion and desorption shrinkage of coalbed methane, the compression of the coal skeleton by gas pressure, and the thermal expansion and contraction effect of temperature.

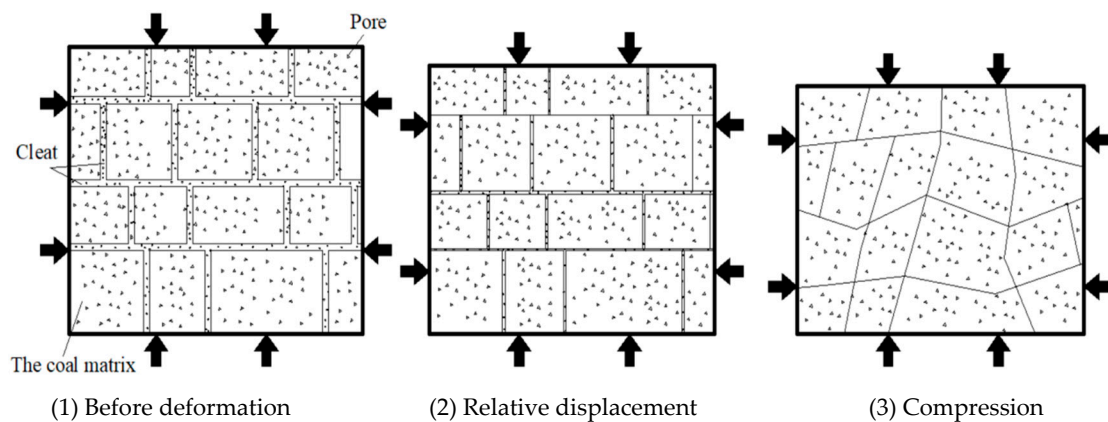


Figure 1. Structural deformation.

This study assumes that the coal seam is thermostatic. Thus, the deformation of the particles under the influence of temperature changes is ignored.

2.2.2. Porosity Mathematical Model

According to the relevant definition of porosity, the porosity change of coal can be expressed as follows:

$$\varphi = \frac{V_p}{V_b} = \frac{V_{p0} + \Delta V_p}{V_{b0} + \Delta V_b} = 1 - \frac{V_{s0} + \Delta V_s}{V_{b0} + \Delta V_b} = 1 - \frac{1 - \varphi_0}{1 + e} \left(1 + \frac{\Delta V_s}{V_{s0}} \right), \quad (1)$$

where φ is coal porosity, φ_0 is the initial porosity of coal, V_p is the pore volume of coal, V_{p0} is the initial pore volume of coal, V_b is the total apparent volume of coal, V_{b0} is the initial total apparent volume of coal, ΔV_p is the variation in the pore volume of coal, ΔV_b is the total apparent volume change in coal, V_s is the volume of the coal skeleton, ΔV_s is the volume variation of the coal skeleton, and e is the volumetric strain of coal.

In the actual state, the volume strain increment of coal particles caused by the bulk deformation of coal particles is mainly composed of three parts. The first part is the strain increment caused by pore gas pressure compressing the coal particles. The second part is the increment in expansion strain caused by coal particles adsorbing the coal bed methane. The third part is the strain increment caused by thermoelastic expansion. The strain increment caused by thermoelastic expansion is zero because we assume that the temperature of the coal seam is constant. In reference to Figure 2, the relationship among the three parts can be expressed as follows:

$$\frac{\Delta V_s}{V_{s0}} = \frac{\Delta V_{sp}}{V_{s0}} + \frac{\Delta V_{sf}}{V_{s0}} + \frac{\Delta V_{st}}{V_{s0}}, \quad (2)$$

where $\frac{\Delta V_{sp}}{V_{s0}}$ is the strain increment caused by pore gas pressure compressing the coal particles, $\frac{\Delta V_{sf}}{V_{s0}}$ is the swelling strain increment caused by coal particles adsorbing the coal bed gas, and $\frac{\Delta V_{st}}{V_{s0}}$ is the strain increment caused by thermal elastic expansion. $\frac{\Delta V_{st}}{V_{s0}}$ is zero because the temperature of the coal seam is assumed to be constant. The total volume strain of coal particle deformation can be expressed as follows:

$$\frac{\Delta V_s}{V_{s0}} = \frac{\Delta V_{sp}}{V_{s0}} + \frac{\Delta V_{sf}}{V_{s0}} = \frac{\varepsilon_p}{1 - \varphi_0} - \frac{\Delta P}{K_s}, \quad (3)$$

where ε_p is the expansion strain generated by the adsorption of gas per unit volume.

$$\varepsilon_p = \frac{2a\rho RT}{3V_m K_s} \ln(1 + bP), \quad (4)$$

where T is the thermodynamic temperature of the coal seam (K), a is the limit adsorption capacity per unit mass of combustibles under a reference pressure (m^3/Mg), b is the adsorption constant (MPa^{-1}), R is the universal gas constant ($R = 8.3143 \text{ J}/(\text{mol}\cdot\text{K})$), ρ is the coal density (kg/m^3), V_m is the molar volume of gas ($22.4 \times 10^{-3} \text{ m}^3/\text{mol}$), and K_s is the volume modulus of the coal skeleton (Pa).

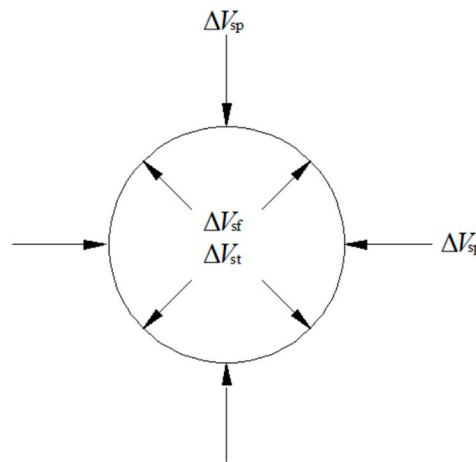


Figure 2. Deformation relationship of coal particles.

Equations (3) and (4) are substituted into Equation (1) to obtain a mathematical model of the dynamic evolution of porosity.

$$\varphi = 1 - \frac{1 - \varphi_0}{1 + e} \left(1 + \frac{\varepsilon_p}{1 - \varphi_0} - \frac{\Delta P}{K_s} \right) = 1 - \frac{1 - \varphi_0}{1 + e} \left(1 + \frac{2a\rho RT}{3V_m K_s (1 - \varphi_0)} \ln(1 + bP) - \frac{P - P_0}{K_s} \right) \quad (5)$$

2.2.3. Permeability Evolution Mathematical Model

Permeability is an important indicator that describes the difficulty of gas migration in gas-bearing coal seams, the permeability of coal seams, and gas drainage difficulty. Therefore, a correct mathematical model of permeability evolution must be established for gas control in coal mines.

The permeability of gas-containing coal is closely related to the stress state of coal. Different stress states cause changes in coal-rock skeleton deformation and pore volume. When porosity changes, permeability also changes. To establish the relationship between coal permeability and porosity, we can refer to the Kozeny–Carman equation [25–27].

$$k = \frac{\varphi}{k_z S_p^2} = \frac{\varphi V_p^2}{k_z A_s^2}, \quad (6)$$

where k is permeability (md), k_z is a dimensionless constant ($k_z = 5$), S_p is the pore surface area per unit pore volume of coal (cm^2), and A_s is the total surface area of coal pore (cm^2).

The permeability in the initial state is assumed to be

$$k_0 = \frac{\varphi V_p^2}{k_z A_s^2}, \quad (7)$$

where k_0 is the initial permeability (md), A_{s0} is the total surface area of the coal pore in the initial state (cm^2).

The total volume of coal and the volume change of a single coal particle are ΔV_b and ΔV_s , respectively, when the initial state changes to a new one. Based on the definition of porosity, the new porosity is

$$\varphi = \frac{V_{p0} + (\Delta V_b - \Delta V_s)}{V_{b0} + \Delta V_b} \quad (8)$$

The new pore surface area can be expressed as follows:

$$S_p = \frac{A_{s0}(1 + \partial)}{V_{p0} + (\Delta V_b - \Delta V_s)}, \quad (9)$$

where ∂ is the increasing coefficient of the pore surface area of coal (%).

For Equations (6) and (7), the ratio of the new permeability to the original permeability is computed by the following:

$$\frac{k}{k_0} = \frac{\varphi S_{p0}^2}{\varphi_0 S_p^2} = \frac{1}{1 + e} \frac{1}{(1 + \partial)^2} \left(\frac{V_{p0} + \Delta V_p}{V_{p0}} \right)^3. \quad (10)$$

The total surface area of the unit volume of coal particles is almost unchanged in the stress and strain process of coal [28]. This occurrence can be ignored. Thus, ∂ is approximately zero. According to [24], Equation (10) can be simplified as follows:

$$\frac{k}{k_0} = \frac{1}{1 + e} \left(\frac{V_{p0} + \Delta V_p}{V_{p0}} \right)^3 = \frac{1}{1 + e} \left(1 + \frac{e}{\varphi_0} - \frac{\Delta V_s}{V_{s0}} \Delta \frac{(1 - \varphi_0)}{\varphi_0} \right)^3. \quad (11)$$

The combination of Equations (3), (4) and (11) can be obtained:

$$k = \frac{k_0}{1 + e} \left[1 + \frac{e}{\varphi_0} + \frac{\Delta P(1 - \varphi_0)}{\varphi_0 K_s} - \frac{2a\rho RT \ln(1 + bP)}{3\varphi_0 V_m K_s} \right]^3. \quad (12)$$

The above equation is a mathematical model for the evolution of the permeability of coal containing gas.

2.3. Effective Stress of Gas-Bearing Coal

Gas-containing coal is a complex deformable pore-fracture dual media. Coal has a strong adsorption capacity for gas and produces a certain adsorption expansion stress, which changes the stress distribution of coal.

Therefore, when studying the problem of fluid–solid coupling of coal containing gas and rock, the relationship between the effective stress of the coal seam and its adsorption-expansion stress should be considered simultaneously. In view of this problem, Wu et al. [29,30] derived the following formula for calculating the expansive stress of coal. The expansion stress formula of coal can be expressed as follows:

$$\sigma_p = E\varepsilon_p = \frac{2a\rho RT(1-2\nu)\ln(1+bP)}{3V_m}, \quad (13)$$

where σ_p is the expansion stress (Pa), ν is the Poisson ratio, and E is the elastic modulus of coal (Pa).

In accordance with the effective stress law of Terzaghi and in consideration of the expansion stress absorbed by coal, the effective stress equation of gas-bearing coal can be expressed as follows:

$$\sigma'_{ij} = \sigma_{ij} - \alpha P\delta_{ij} - \sigma_p\delta_{ij}, \quad (14)$$

where σ'_{ij} is the effective stress of gas-bearing coal (MPa), σ_{ij} is the overall stress of gas-containing coal (MPa), and α is the Biot coefficient.

2.4. Establishment of a Fluid–Solid Coupling Model of Gas-Bearing Coal

2.4.1. Gas Content Equation

The existing mine gas in the coal bed occurs mostly in free, adsorption, and dissolved states. The dissolved gas content is not considered in this study because the amount is notably small. The gas content is the sum of the free-state and adsorbed-state gas contents. The adsorption gas content accounts for more than 90% of the total, and the content of adsorption gas is related to moisture, coal ash, and gas pressure. The free gas content mainly depends on coal porosity and the magnitude of gas pressure. According to previous research and the modified Langmuir adsorption equilibrium equation, the gas content of a coal seam can be obtained as follows [31]:

$$Q = \left(\frac{abcP}{1+bP} + \varphi \frac{P}{P_n} \right) \rho_n, \quad (15)$$

where P_n is the gas pressure under standard conditions ($P_n = 0.10325$ MPa), and ρ_n is the coalbed methane density under standard conditions (kg/m^3).

In the above equation,

$$c = \rho \frac{1-A-M}{1+0.31M},$$

where Q is the gas content (kg/m^3), c is the coal quality correction parameter (kg/m^3), A is the ash content of coal (%), and M is the coal moisture (%).

2.4.2. Stress Field Equation of Gassy Coal

Assuming that the gas-bearing coal is an isotropic linear elastic medium, the stress field changes obey the following equation.

(1) Balance equation

$$\sigma_{ij,j} + F_i = 0 (i, j = 1, 2, 3), \quad (16)$$

where F_i is the bulk stress (N/m^3).

According to the effective stress Equation (14) of gas-bearing coal, the equilibrium differential equation expressed by effective stress is obtained by the introduction of Equation (16). Then the equilibrium differential equation can be expressed as follows:

$$\sigma'_{ij,j} + (\alpha P \delta_{ij})_{,j} + (\sigma_p \delta_{ij})_{,j} + F_i = 0 \quad (17)$$

(2) Geometric equation

In the spatial distribution of gas-bearing coals, let $u(x, y, z)$, $v(x, y, z)$, and $w(x, y, z)$ be the displacement components in directions x , y , and z , respectively, and continuous single-valued functions of coordinates. Then, the strain and displacement components satisfy the following geometric equations, which can be expressed as tensor symbols.

$$\varepsilon_{ij} = \frac{1}{2}(u_{i,j} + u_{j,i}) \quad (i, j = 1, 2, 3) \quad (18)$$

(3) Constitutive equation of gas-bearing coal

The constitutive equation of gas-bearing coal describes the relationship between the stress and strain of coal. The constitutive relationship in this study is based on the strains caused by the adsorption expansion of gas-bearing coal, compression of the coal particle body, and rock stress.

The linear strain caused by gas adsorption by coal particles is as follows:

$$\varepsilon_{PX} = \frac{2a\rho RT}{9V_m K_s} \ln(1 + bP) \quad (19)$$

The linear compression strain of coal particles caused by the change in pore gas pressure is as follows:

$$\varepsilon_{PY} = -\frac{\Delta P}{3K_s}. \quad (20)$$

According to Hooke's law, the strain due to crustal stress is computed using the following:

$$\varepsilon_D = \frac{1}{2G} \left(\sigma' - \frac{v}{1+v} \Theta' \right). \quad (21)$$

According to the above expressions, the total strain of gas-bearing coal is as follows

$$\varepsilon = \varepsilon_{PX} + \varepsilon_{PY} + \varepsilon_D = \frac{2a\rho RT}{9V_m K_s} \ln(1 + bP) - \frac{\Delta P}{3K_s} + \frac{1}{2G} \left(\sigma' - \frac{v}{1+v} \Theta' \right). \quad (22)$$

By using the above formula as a reference, the following equation can be derived.

$$\sigma' = 2G\varepsilon + \frac{v}{1+v} \Theta' - 2G \left(\frac{2a\rho RT \ln(1 + bP)}{9V_m K_s} - \frac{\Delta P}{3K_s} \right) \quad (23)$$

where G is the shear modulus (MPa), and Θ' is the effective volume stress.

The following equation can be obtained by arranging Equation (23) after introducing the Lamé constant.

$$\sigma' = 2G\varepsilon + \lambda e + \frac{2G\Delta P}{3K_s} - \frac{4Ga\rho RT \ln(1 + bP)}{9V_m K_s}, \quad (24)$$

where λ is the Lamé constant.

Assuming that the coal is a linear elastic medium, the constitutive equation of gas-bearing coal-rock deformation conforms to Hooke's law, as follows:

$$\sigma'_{ij} = \lambda e \delta_{ij} + 2G\varepsilon_{ij}. \quad (25)$$

According to the stress–strain relationship of coal in Equation (32) and combined with the above formula, the effective stress constitutive equation of gas-bearing coal expressed in tensor form is derived as follows:

$$\sigma'_{ij} = \lambda e \delta_{ij} + 2G \varepsilon_{ij} + \frac{2G \Delta P}{3K_s} \delta_{ij} - \frac{4Ga \rho RT \ln(1 + bP)}{9V_m K_s} \delta_{ij}. \quad (26)$$

(4) Stress field equation of gas-bearing coal

Substituting Equation (26) into Equation (17) yields the following:

$$G \sum_{j=1}^3 \frac{\partial^2 u_i}{\partial x_j^2} + \frac{G}{1-2\nu} \sum_{j=1}^3 \frac{\partial^2 u_i}{\partial x_i \partial x_j} + \left[\alpha + \frac{2G}{3K_s} + \left(\frac{1-2\nu}{V_m} - \frac{2G}{3V_m K_s} \right) \frac{2ab \rho RT}{3(1+bP)} \right] \frac{\partial P}{\partial x_i} + F_i = 0. \quad (27)$$

This formula is the fluid–solid coupling stress field equation of gas-containing coal, and the deformation field of gas-bearing coal is represented by displacement. The variation of the strain field of gas-containing coal caused by crustal stress, gas adsorption by coal particles, and gas pressure change are considered in the equation.

2.4.3. Fluid–Solid Coupling Gas Seepage Equation of Gas-Bearing Coal

(1) Gas flow equation

The previous experimental results reveal that when gas migrates in low-permeability gas-bearing coal seams, the gas molecules near the surface of the coal wall show the phenomenon of non-zero velocity, which does not conform to Darcy's law [32]. This occurrence is called the slippage effect or Klinkenberg effect in seepage mechanics. Its permeability can be expressed as follows:

$$k = k_g \left(1 + \frac{4\omega \lambda_1}{r} \right) = k_g \left(1 + \frac{m}{P} \right), \quad (28)$$

where k_g is the Klinkenberg permeability, ω is the scale factor, λ_1 is mean free path of gas molecules, r is the average pore radius, m is the Klinkenberg coefficient (MPa), and ∇P is the gas pressure gradient in the coal seam (Pa/m).

Therefore, when the Klinkenberg effect is considered, the equation of gas flow in the coal seam can be expressed by the following:

$$q = -\frac{k_g}{\mu} \left(1 + \frac{m}{P} \right) \nabla P, \quad (29)$$

where q is the velocity vector of gas flow (m/s), and μ is the gas dynamic viscosity (1.08×10^{-5} Pa·s).

(2) Continuity equation

According to the hypothesis, if the model is isolated from the outside and no exchange of substance and energy in any form occurs, the gas flow in the coal seam will conform to the law of conservation of mass, expressed in the form of a differential equation:

$$\frac{\partial Q}{\partial t} + \nabla \cdot (\rho_g q) = I, \quad (30)$$

where Q is the gas content in coal, ρ_g is the gas density when the gas pressure is P (kg/m^3), and I is the source sink term.

(3) Gas seepage field equation of gas-bearing coal

According to the state equation of coalbed methane in [33], the gas content equation (15), and the gas flow equation (29), the equation of gas seepage flow field can be obtained by combining them with Equation (30). The result is as follows:

$$\frac{M_g}{RT} \left[\varphi + \frac{abcP_n}{(1+bP)^2} + \frac{(1-\varphi_0)P}{(1+e)K_s} - \frac{2ab\rho RTP}{3V_m K_s(1+bP)(1+e)} \right] \frac{\partial P}{\partial t} - \frac{M_g P}{RTZ} \left[\frac{k_g}{\mu} \left(1 + \frac{m}{P} \right) \nabla P \right] = - \frac{M_g P}{RT} \cdot \varphi \frac{\partial e}{\partial t}, \quad (31)$$

where M_g is the molar mass of gas (kg/mol). Z is the gas compressibility factor, and its value is approximately 1 in the case of a small temperature difference.

In summary, Equations (5), (12), (27), and (30) constitute a fluid–solid coupling model of gas-bearing coal.

3. Numerical Simulation of the Model and Analysis of Its Results

Deduction and analysis show that the fluid–solid coupling mathematical model of gas-bearing coal is a complex nonlinear equation group. The coupled numerical solution requires the use of a numerical method and COMSOL Multiphysics simulation software.

3.1. Geometric Model Establishment

The geometric model starts from the 370 m position of the transportation lane on the 14221 working face of Xin'an coal mine. The coal mine is an experimental site for determining the effective influence radius of the drilling borehole down the seam. The main mining coal seam is No. 21 coal, and the average coal seam thickness is 4.22 m. The coal seam has a simple structure and extremely low mechanical strength. The soft coal structure is developed and generally classified as classes III–V. The coal is powdery and easily polluted.

The size of the geometric model is 14 m × 14.22 m. Figure 3 shows the geometric diagram of the model. The model is divided into three layers, in which the coal seam is located in the two rock layers, the thickness is 4.22 m, and the upper part is loaded with a stable load of 11.7 MPa. The borehole is located in the middle of the model and has a diameter of 0.089 m and a negative pressure of 13 kPa. The initial gas pressure in the coal seam is 0.9 MPa, and the gas only migrates in the coal seam. The initial time is $t = 0$ day, and the simulation time is 100 days.

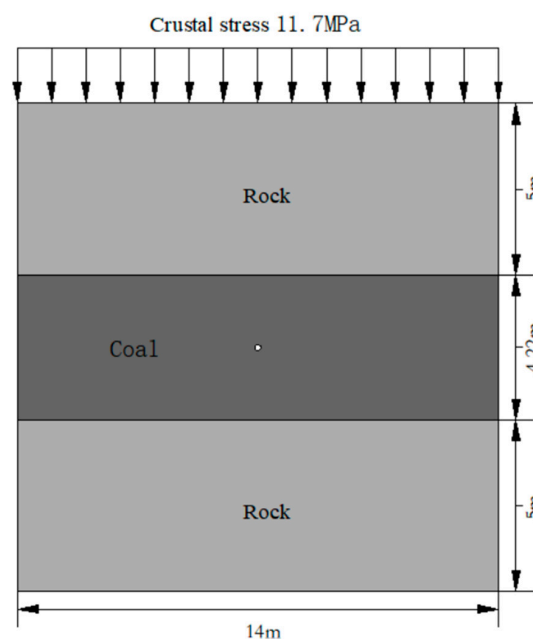


Figure 3. Coal and gas coupling geometric model.

According to the field measurement, the drainage radius of the drilling borehole down the seam is the effective extraction radius of 1.5–1.8 m when the gas is extracted for 30 days. The measured drainage radius of the mine is the effective extraction radius of 3 m when the gas is extracted for 80 days. These data are used to verify the practical application value of the model.

3.2. Model Parameters

Table 1 shows the relevant parameters of the fluid–solid coupling model of gas-bearing coal.

Table 1. Material parameters of gas-bearing coal.

Parameter Name	Symbol	Unit	Numerical Value
Coal density	ρ	(kg·m ⁻³)	1400
Poisson's ratio of coal	ν	/	0.32
Elastic modulus of coal	E	GPa	2.74
Initial porosity of coal	φ_0	/	0.0485
Initial permeability of coal	k_0	m ²	4.59×10^{-17}
Adsorption constant a	a	m ³ ·Mg ⁻³	35
Adsorption constant b	b	MPa ⁻¹	0.762
Gas dynamic viscosity coefficient	μ	Pa·s	1.08×10^{-5}
Moisture	M	%	0.64
Ash	A	%	13.81
Gas density in standard state	ρ_g	kg·m ⁻³	0.716
Initial gas pressure	P ₀	MPa	0.9
Drainage negative pressure	P ₁	Pa	13,000

3.3. Input of the Mathematical Model

The mathematical model in Chapter 2 is inputted into the COMSOL Multiphysics numerical simulation software (COMSOL Multiphysics 5.4.0.388, COMSOL Inc., Stockholm, Sweden, 1986) to verify the rationality of the mathematical model. Figure 4 shows the specific input.

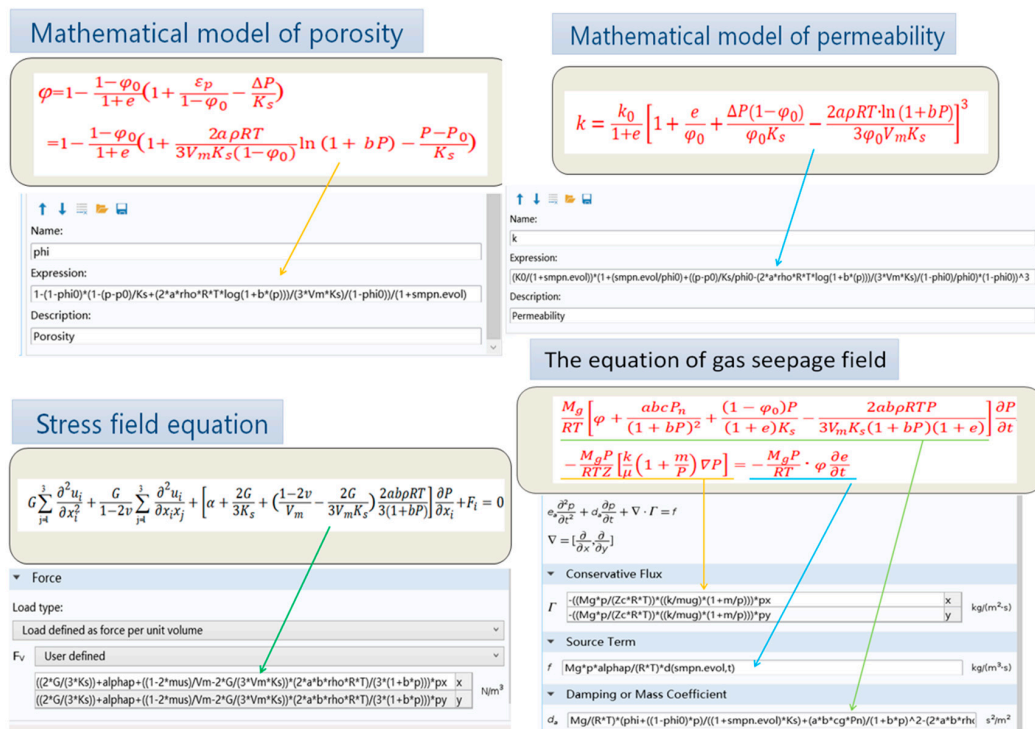


Figure 4. Mathematical model input.

3.4. Initial Conditions and Boundary Conditions

(1) Initial conditions of gas seepage flow field

$$P|_{t=0} = P_0, \quad (32)$$

where P_0 is the initial gas pressure in the coal seam.

(2) Boundary conditions

When $t = 0$, the displacement boundary conditions of the model are:

$$u|_L = u_0, \quad (33)$$

where u_0 is the initial displacement on the boundary.

(3) Stress boundary conditions

$$\rho_{ij}n_j = f_i, \quad (34)$$

where f_i is the surface force on the boundary.

$$q|_L = q_m, \quad (35)$$

where q_m is the gas flow on the boundary.

The roof and floor of the coal seam in the model are rock layers with poor gas permeability. Thus, both are assumed to be flow boundaries, and the flux is zero.

(4) Pressure boundary conditions

$$P|_L = P_m, \quad (36)$$

where P_m is the gas pressure on the boundary.

3.5. Analysis of the Numerical Simulation Results of the Model

Figure 5 shows the distribution of instantaneous gas pressure during the fluid–solid coupling deformation of coal. Figure 6 shows the contour figure of gas pressure for 30 and 80 days of extraction. The graph indicates that the maximum gas pressure in the coal seam is distributed on both sides of the geometric model. When $t = 1$ day, the gas pressure is 0.6 MPa at 0.32 m away from the drilling hole. With the increase in extraction time, the gas pressure around the borehole decreases gradually. When $t = 30$ days, the gas pressure is 0.6 MPa at 1.73 m from the drilling hole. When $t = 80$ days, the gas pressure is 0.6 MPa at 2.76 m away from the drilling hole.

According to Henan's regulations on the prevention and control of coal and gas, the critical value of gas pressure should not be more than 0.6 MPa. This value can be used as a reference for the effective extraction radius of extraction boreholes. The numerical simulation results show that when $t = 30$ days, the effective extraction radius of the extraction borehole is 1.73 m. When $t = 80$ days, the effective extraction radius of the extraction borehole is 2.76 m. The drilling drainage radius measured by Henan University of Science and Technology is 1.5–1.8 m for 30 days and 3 m for 80 days [34,35]. The numerical simulation results are basically consistent with the measured results, indicating their strong practical application value.

Figure 7 shows the instantaneous gas pressure evolution curve of the fluid–solid coupling of coal during deformation. The graph shows that the closer the distance from the drainage hole, the faster the gas pressure drops and the more noticeable the pressure relief effect is. The pressure relief of coalbed methane is a nonlinear process. Within a certain limit, the change in gas pressure gradient decreases with the increase in time.

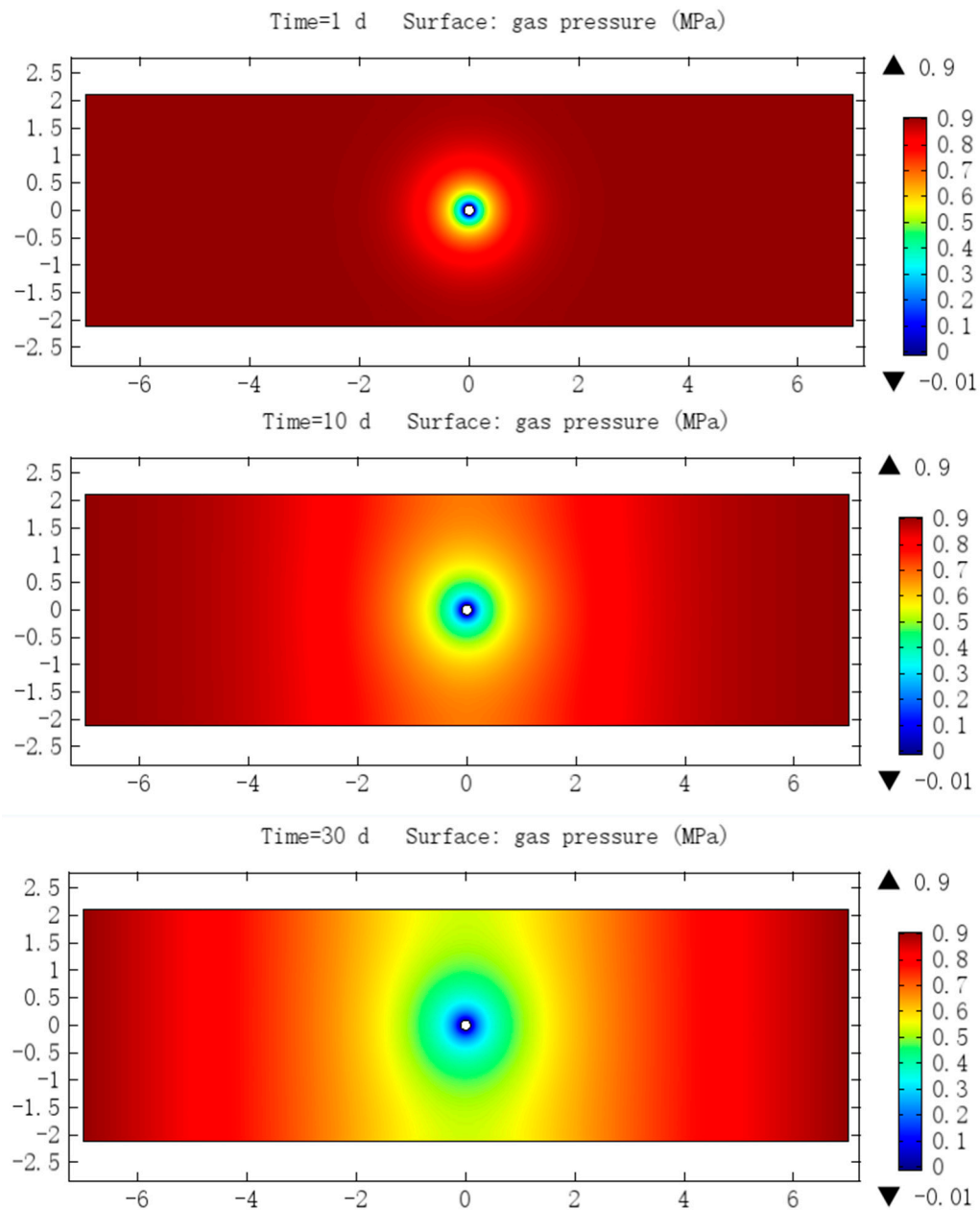


Figure 5. Cont.

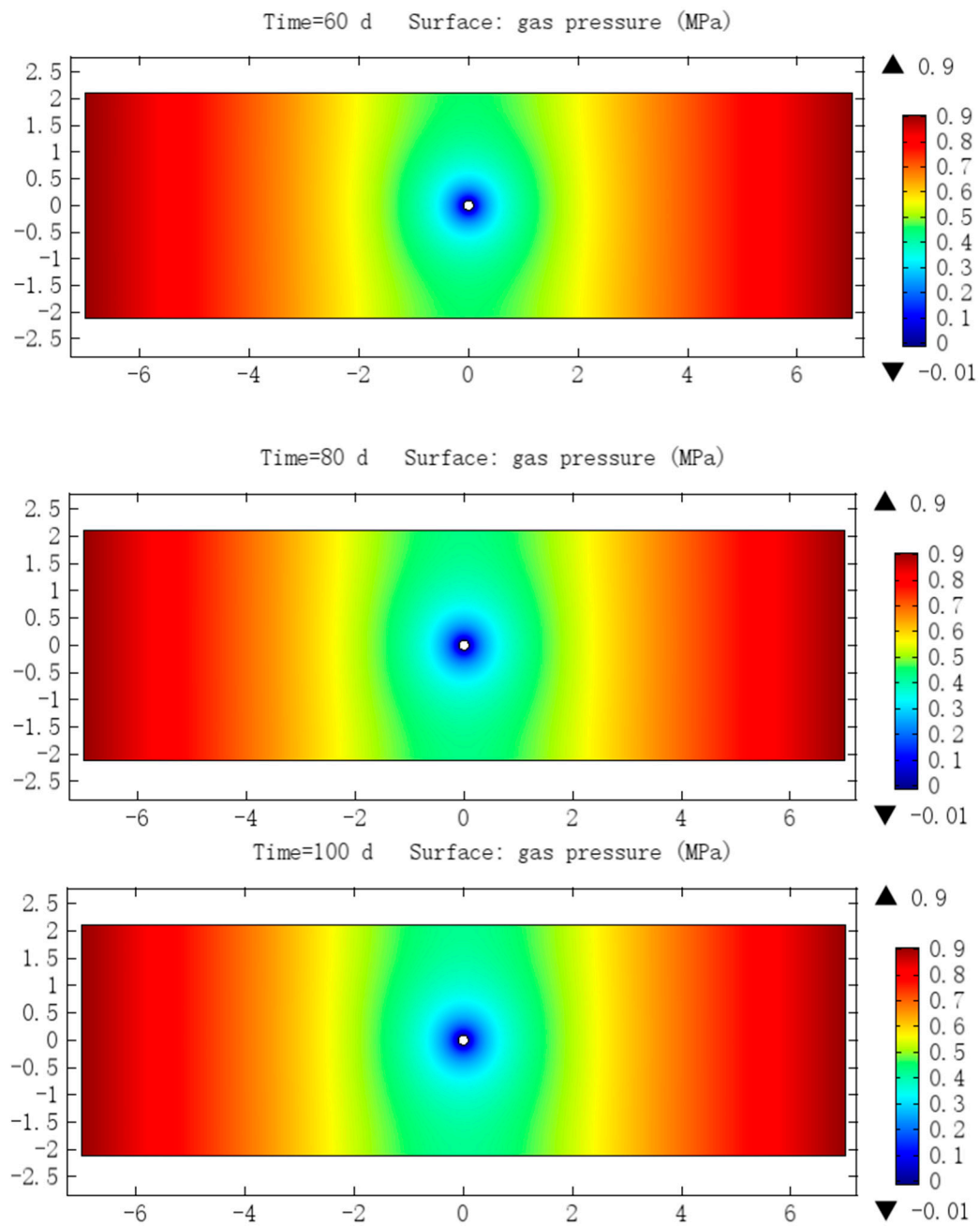


Figure 5. Gas pressure profile at different times.

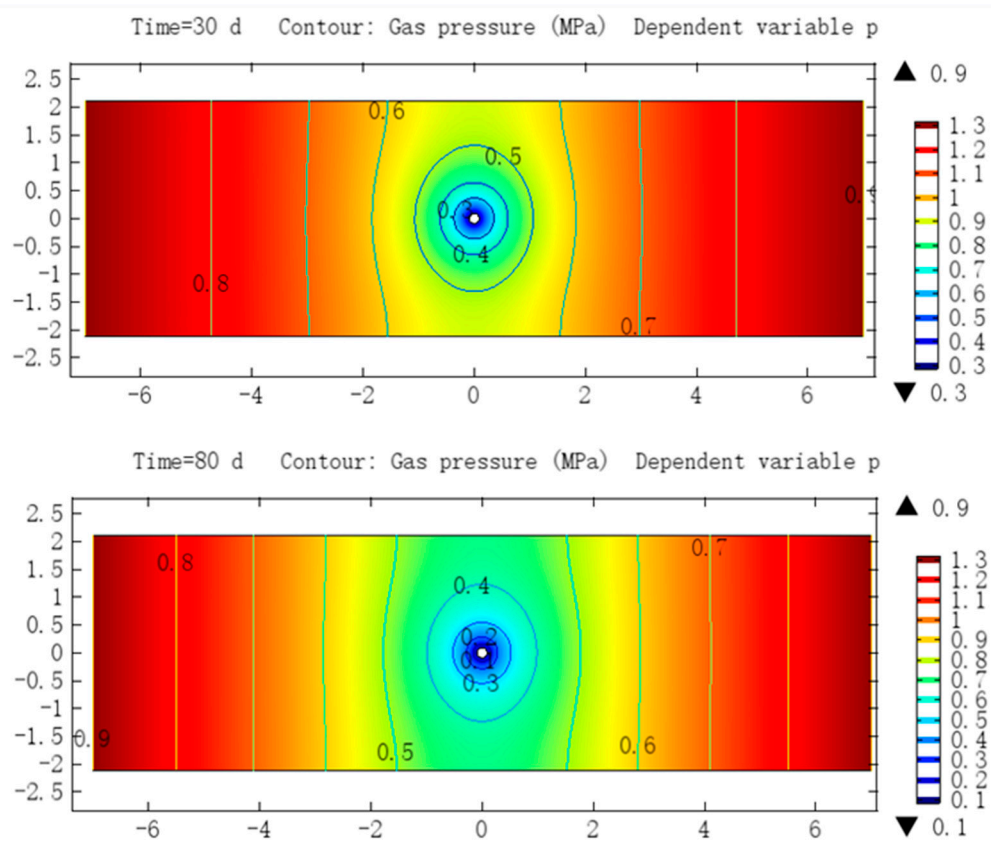


Figure 6. Contour maps of gas pressure at different times.

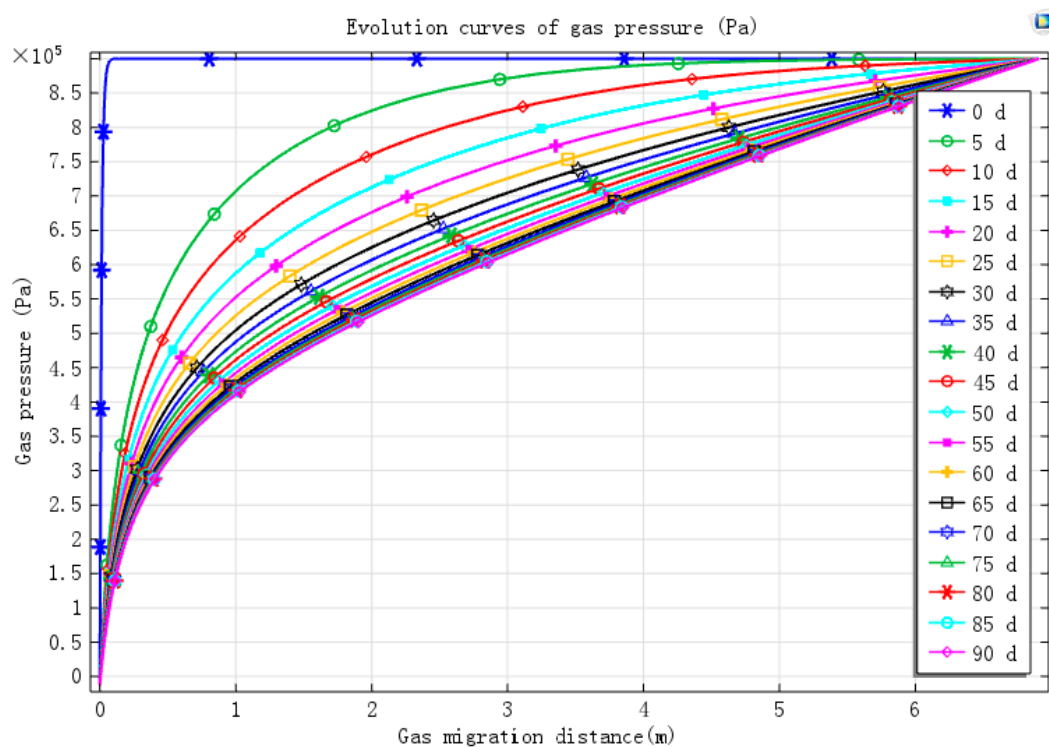


Figure 7. Evolution curves of gas pressure.

Figures 8 and 9 show the evolution curves of the porosity and permeability of coal around the borehole after drilling along the seam, respectively. The graph shows that the minimum values of porosity and permeability is lower than the initial ones at the initial state on day 0 because of the stress concentration area around the drill hole. In this area, the pores are compressed, the pore channel of gas migration and production is small, and the permeability is reduced. With the increase in extraction time, the closer the distance from the drilling hole, and the larger the values of porosity and permeability of coal are. Coal porosity and permeability increase with the increase in time, but the rate of increase declines gradually. The changing trend of permeability is almost similar to that of porosity because the closer the distance from the borehole, the more evident the coal disruption by artificial disturbance is. The coal rock breaks and forms a new pore, and its permeability increases. After gas drainage, the coal gas pressure near the extraction borehole, the gas content, and the gas adsorbed by coal particles are reduced. The coal body shrinks, coal pores and fissures are developed, and the permeability increases. The shrinkage and deformation of the coal-rock matrix are also the main factors determining coal adsorption characteristics. Although the regional pressure of the coal seam cannot be reduced, the gas dissolution in coal induces the shrinkage of the coal matrix, which enlarges the fissures and creates internal ones in the coal seam. In this way, coal porosity, the channel of gas migration and output, and permeability increase.

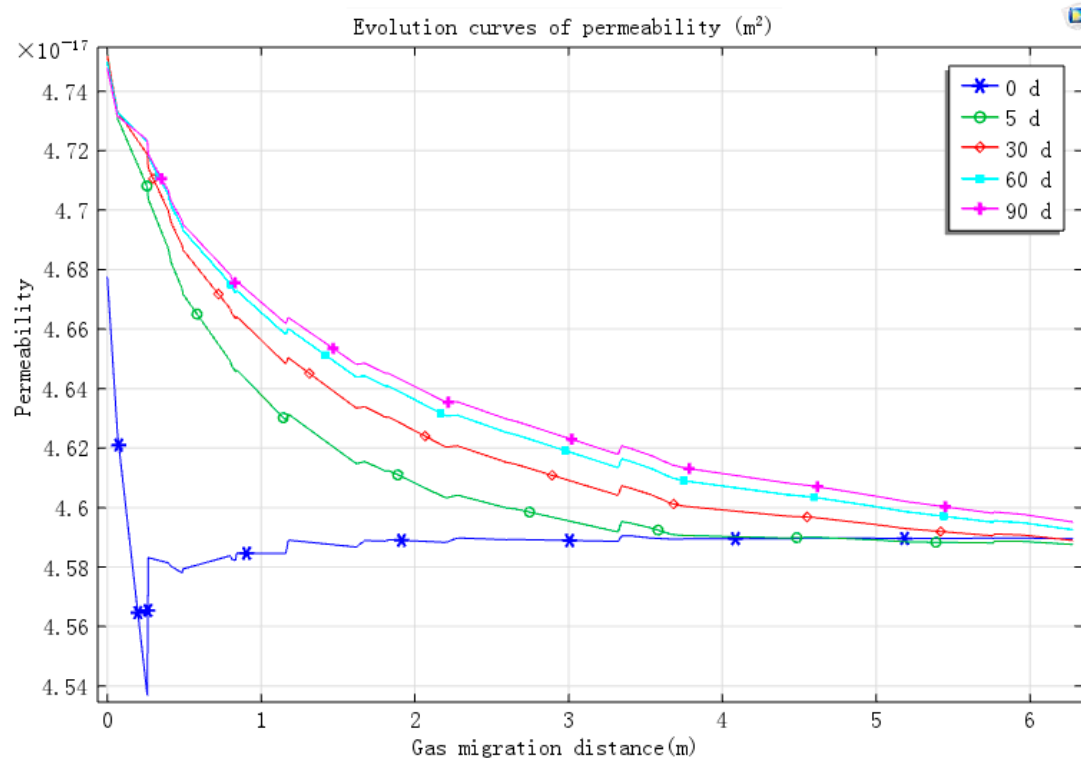


Figure 8. Evolution curves of porosity.

Figures 8 and 9 show that the porosity and permeability of coal also increase from both sides of the coal seam to the direction of the extraction boreholes, respectively. The closer to the extraction boreholes, the greater the increase in range. With the passage of time, the increase rate of permeability and porosity decreases significantly. This situation is mainly due to the artificial disturbance around the drilling hole. The coal becomes unstable and pressure-relieved, and pores and cracks increase. With the decrease in gas content in the coal seam pore, the effective stress of coal increases, the coal compresses, and porosity and permeability decrease. At the same time, the absorbed gas is constantly used to supply pore gas, and the volume shrinkage of coal particles increases the porosity, which affects

the increase in coal permeability. With the continuation of extraction time, the increase in porosity and permeability of coal decreases under the two effects.

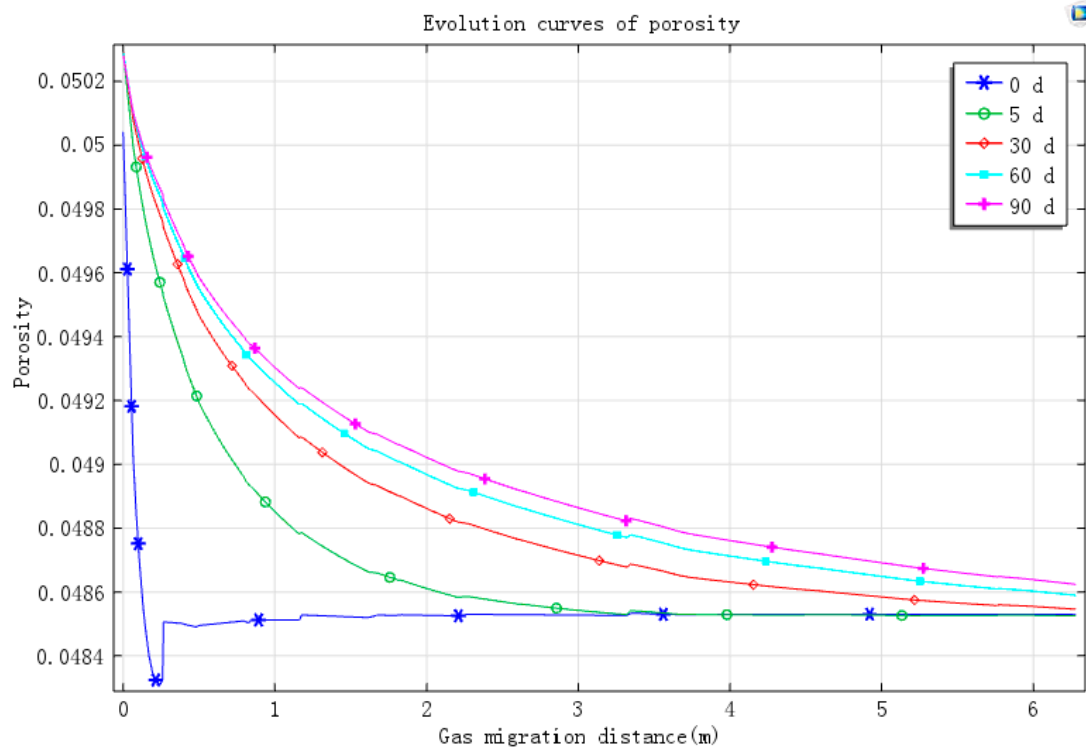


Figure 9. Evolution curves of permeability.

3.6. Discussion

After establishing the fluid–solid coupling model of gas-bearing coal, the model’s field practicability needs to be verified. A good model should be applied to practical applications to reflect its importance and guiding significance for practical design and production work. The SF6 gas tracing method is mainly used to measure the effective extraction radius of the bedding borehole in this coal mine. This method overcomes many of the limitations of traditional measuring methods, such as numerous drilling holes, complicated working procedures, high requirement for sealing quality, long time, and large deviation, leading to a highly accurate, reliable, and simple measurement [36]. The measured effective extraction radius is 1.5–1.8 m at 30 days of extraction. The relevant parameters of the measured coal seams are inputted into the mathematical model, and the coupled numerical solution is calculated with COMSOL Multiphysics simulation software. The calculation results show that the effective extraction radius is 1.73 m. Afterward, the effective extraction radius is measured independently in the mine. The measured effective extraction radius is 3 m at 80 days, and the effective extraction radius is 2.76 m by numerical simulation.

A comparison with the results of field measurement shows that the numerical simulation findings of this model are close to actual conditions. The results provide reference values for the rational layout of extraction boreholes in coal mines. Based on the fluid–solid coupling equation, the effective extraction radius simulation of drilling boreholes along the seam reveals the gas pressure distribution state at different extraction times. This condition eliminates the blank belt of gas drainage with the time effect, changes the current disadvantage of the restricted effective radius test of gas extraction by many factors, and ensures the safe production of mines to a great extent. Moreover, the process of establishing the model reveals the mechanism of gas migration in the coal seam and describes factors one by one from the perspectives of coal pore, coal particle adsorption expansion deformation, compression deformation, stress field, and gas seepage flow field. Then, a relatively complete practical

mathematical model is obtained. This model considers the effects of adsorption expansion and the Klinkenberg effect on gas migration in coal seams. The model improves the application of fluid–solid coupling theory in coal. The numerical simulation results show the dynamic changes in gas pressure in the coal seam and the dynamic evolution of porosity and permeability. The model can simulate the dynamic evolution law of coalbed methane in the corresponding coal seam of the coal mine based on different coal seam parameters, such as the influence of different types of water and ash on gas migration and various extraction negative pressures on the drainage effect. The numerical simulation shows the extraction effect and scope of gas drainage boreholes and provides important theoretical support and basis for the rational optimization and layout of gas drainage boreholes in mines.

4. Conclusions

The mathematical model combines the findings of previous studies on the effects of adsorption expansion and the Klinkenberg effect on gas migration in coal seams. On the basis of the basic definitions of porosity and permeability, a mathematical model of dynamic evolution of porosity and permeability is derived. On the basis of fluid–solid coupling theory, a mathematical model of fluid–solid coupling with gas-bearing coal is established.

According to the results of the numerical simulation, when $t = 30$ days and $t = 80$ days, the effective extraction radius of the bedding borehole reaches 1.73 m and 2.76 m, respectively. The simulation results are consistent with the actual measured extraction radius values. Figure 5 shows the effect of gas pressure reduction around the borehole with the continuous change in simulation time. The gas pressure decreases, and the porosity and permeability of coal increase with the increase in gas extraction time. In addition, the growth rate of permeability and porosity decreases with the increase in gas extraction time. These results are consistent with the field permeability test law and can be used as reference to further understand the mechanism of gas extraction and mine gas control. The research results also have theoretical significance and practical application value.

The dynamic evolution mathematical model of fluid–solid coupling for gas bearing coal can reflect the coalbed methane migration in a mining area of the mine through the coal seam parameters measured by coal miners. According to the simulation results of the model, the effective extraction radius of the borehole can be predicted. Thus, the extraction borehole can be optimized and reasonably arranged for safety reasons and scientific purposes, to effectively control mine gas, and to provide strong support for decision-makers as they formulate efficient coal mining schemes.

Although the model is an extension of the theory of fluid–solid coupling, its simulation results can be suitable for field applications. However, several problems should be considered in the multi-field coupling model, thus indicating the need for further research and improvement. For example, with the increase in mining depth, the influence of temperature on gas adsorption and migration in the coal seam considerably influences gas extraction. Another example is the influence of movable and residual water in the coal seam on expansion stress in the gas-bearing coal seam [37]. Studying these problems is crucial for the further improvement of the model.

Author Contributions: S.H. developed the analytical models, analyzed the data, and wrote the paper; X.L. (Xianzhong Li) gave valuable advice and contributed to the manuscript editing. X.L. (Xiao Liu) provided financial support for this paper. All authors have read and agreed to the published version of the manuscript.

Funding: This research was funded by Project of science and technology of Henan Province in 2015 (152102310095) and Project of science and technology of Jiaozuo science and Technology Bureau (Applied Basic Research) (2014400018).

Acknowledgments: This work was financially supported by the National Natural Science Foundation of Henan Science and Technology Project in 2015 (152102310095) and Science and Technology Research Project of Jiaozuo Science and Technology Bureau (Applied Basic Research) (2014400018). The support provided by these entities is gratefully acknowledged. I would also like to thank Liu and Li for their earnest guidance.

Conflicts of Interest: The authors declare no conflict of interest.

References

1. Liu, C.; Zhu, Q.; Wei, F.; Rao, W.; Liu, J.; Hu, J.; Cai, W. An integrated optimization control method for remanufacturing assembly system. *J. Clean. Prod.* **2019**, *248*, 119261. [\[CrossRef\]](#)
2. Liu, C.; Zhu, Q.; Wei, F.; Rao, W.; Liu, J.; Hu, J.; Cai, W. A review on remanufacturing assembly management and technology. *Int. J. Adv. Manuf. Technol.* **2019**, *105*, 4797–4808. [\[CrossRef\]](#)
3. Cai, W.; Liu, C.; Jia, S.; Chan, F.T.; Ma, M.; Ma, X. An emergy-based sustainability evaluation method for outsourcing machining resources. *J. Clean. Prod.* **2019**, *245*, 118849. [\[CrossRef\]](#)
4. Hou, Z.; Xie, H.; Zhou, H.; Were, P.; Kolditz, O. Unconventional gas resources in China. *Environ. Earth Sci.* **2015**, *73*, 5785–5789. [\[CrossRef\]](#)
5. Zhu, W.C.; Wei, C.H.; Liu, J.; Xu, T.; Elsworth, D. Impact of gas adsorption induced coal matrix damage on the evolution of coal permeability. *Rock Mech. Rock Eng.* **2013**, *46*, 1353–1366. [\[CrossRef\]](#)
6. Sommerton, W.J.; Soylemezoglu, I.M.; Dudley, R.C. Effect of stress on permeability of coal. *Int. J. Rock Mech. Min. Sci. Geomech. Abstr.* **1975**, *12*, 129–145. [\[CrossRef\]](#)
7. Brace, W.F. A note on permeability changes in geologic material due to stress. *Pure Appl. Geophys.* **1978**, *116*, 627–632. [\[CrossRef\]](#)
8. McKee, C.R.; Bumb, A.C.; Koenig, R.A. Stress-dependent permeability and porosity of coal. In *Rocky Mountain Association of Geologists Guidebook*; Fassett, J.E., Ed.; Rocky Mountain Association of Geologists: Denver, CO, USA, 1988; pp. 143–153.
9. Enever, J.R.E.; Henning, A. The relationship between permeability and effective stress for Australian coal and its implications with respect to coalbed methane exploration and reservoir model. In *Proceedings of the 1997 International Coalbed Methane Symposium*; University of Alabama: Tuscaloosa, AL, USA, 1997; pp. 13–22.
10. Sun, P.D. Study on the Flow Law of coal seam gas flow field. *J. Coal Mine* **1987**, *12*, 74–82.
11. Sun, P.D. Research on gas dynamics model. *Coalf. Geol. Explor.* **1993**, *21*, 32–40.
12. Sun, P.D. Coal gas dynamics and its applications. *Sci. Geol. Sin.* **1994**, *3*, 66–72.
13. Li, X.C.; Guo, Y.Y.; Wu, S.Y. The relationship among coal adsorption swelling deformation, porosity and permeability. *J. Taiyuan Univ. Technol.* **2005**, *36*, 264–265.
14. Harpalani, S.; Chen, G. Estimation of Changes in Fracture Porosity of Coal with Gas Emission. *Fuel* **1995**, *75*, 1491–1498.
15. Yunqi, T.A.O.; Jiang, X.U.; Shuchun, L.I.; Shoujian, P.E.N.G. Advances in study on seepage flow property of coalbed methane. *Coalf. Geol. Surv.* **2009**, *37*, 1–5.
16. Yin, G.Z.; Wang, D.K.; Zhang, D.M.; Hang, G. Solid-gas coupling dynamic model and numerical simulation of coal containing gas. *Rock Soil Mech.* **2008**, *30*, 1431–1435.
17. Zhu, W.C.; Liu, J.; Sheng, J.C.; Elsworth, D. Analysis of coupled gas flow and deformation process with desorption and Klinkenberg effects in coal seams. *Int. J. Rock Mech. Min. Sci.* **2007**, *44*, 971–980. [\[CrossRef\]](#)
18. Xia, T.Q.; Gao, F.; Kang, J.H.; Wang, X.X. A fully coupling coal–gas model associated with inertia and slip effects for CBM migration. *Environ. Earth Sci.* **2016**, *75*, 582. [\[CrossRef\]](#)
19. Lu, S.Q.; Cheng, Y.P.; Li, W. Model development and analysis of the evolution of coal permeability under different boundary conditions. *J. Nat. Gas Sci. Eng.* **2016**, *31*, 129–138. [\[CrossRef\]](#)
20. Chen, Y.; Xu, J.; Peng, S.; Yan, F.; Fan, C. A Gas-Solid-Liquid Coupling Model of Coal Seams and the Optimization of Gas Drainage Boreholes. *Energies* **2018**, *11*, 560. [\[CrossRef\]](#)
21. Liu, Y.B.; Cao, S.G.; Li, Y.; Wang, J.; Guo, P.; Xu, J.; Bai, Y.J. Experimental study on the deformation effect of coal adsorptive expansion. *J. Rock Mech. Eng.* **2010**, *29*, 2484–2491.
22. Yang, C.; Li, X.; Ren, Y.; Zhao, Y.; Zhu, F. Statistical analysis and countermeasures of gas explosion accident in coal mines. *Procedia Eng.* **2014**, *84*, 166–171.
23. Xie, Z.C.; Zhang, D.M.; Song, Z.L.; Li, M.H.; Liu, C.; Sun, D.L. Optimization of Drilling Layouts Based on Controlled Presplitting Blasting through Strata for Gas Drainage in Coal Roadway Strips. *Energies* **2017**, *10*, 1228. [\[CrossRef\]](#)
24. Tao, Y.Q. THM coupling model of gas-bearing coal and Simulation of coal and gas outburst. Ph.D. Thesis, Chongqing University, Chongqing, China, 2009.
25. Guo, P.; Cao, S.G.; Zhang, Z.G.; Li, Y.; Liu, Y.B.; Li, Y. Solid-gas coupling mathematical model and numerical simulation of gas-bearing coal. *J. Coal Sci.* **2012**, *37*, 330–336.

26. Ettinger, I.L. Swelling stress in the gas-coal system as an energy source in the development of gas bursts. *Sov. Min. Sci.* **1979**, *15*, 494–501. [[CrossRef](#)]
27. Lu, P.; Shen, Z.; Zhu, G.W. Effective stress and mechanical deformation failure characteristics of coal containing gas. *J. Univ. Sci. Technol. China* **2001**, *3*, 687–693.
28. Lu, P.; Shen, Z.W.; Zhu, G.W.; Fang, E.C. Percolation Characterization and Experimental Study of Rock Sample in the Whole Process of Stress and Strain. *J. China Univ. Sci. Technol.* **2002**, *32*, 678–684.
29. Wu, S.Y.; Zhao, W. Effective stress analysis of coal containing adsorbed coalbed methane. *J. Rock Mech. Eng.* **2005**, *24*, 1674–1678.
30. Wu, S.Y.; Zhao, W. Analysis of effectives in adsorbed methane-coal system. *Chin. J. Rock Mech. Eng.* **2005**, *24*, 1674–1678.
31. Sun, P. *Introduction to Multiphysical Field Coupling Model. and Numerical Simulation*; China Science and Technology Press: Beijing, China, 2007.
32. Zhou, S.; Lin, B.Q. *Theory of Coal Seam Gas Occurrence and Flow*; Coal Industry Press: Beijing, China, 1990.
33. Yue, G.W.; Liu, J.; Wang, Z.F. Study on Coal Seam Gas Content Based on Real Gas State Equation. *J. Saf. Environ.* **2014**, *14*, 73–77.
34. Liu, S.J.; Ma, G.; Lu, J.; Lin, B.Q. Relative pressure determination technology for effective radius found on gas content. *J. China Coal Soc.* **2011**, *36*, 1715–1719.
35. Liu, Q.Q.; Cheng, Y.P.; Wang, H.F.; Liu, H.Y.; Liu, J.J. Numerical Resolving of Effective Methane Drainage Radius in Drill Hole along Seam. *Coal Min. Technol.* **2012**, *17*, 5–7.
36. Chen, J.Y.; Ma, P.L.; Kong, Y.H.; Ma, C. SF₆ gas tracer method for determining effective radius of gas drainage in boreholes. *Saf. Coal Mines.* [[CrossRef](#)]
37. Hu, Y.; Shao, Y.; Lu, Y.; Zhang, Y.F. Experimental study on occurrence models of water in pores and the influencing to the development of tight gas reservoir. *Nat. Gas Geosci.* **2011**, *22*, 176–181.



© 2020 by the authors. Licensee MDPI, Basel, Switzerland. This article is an open access article distributed under the terms and conditions of the Creative Commons Attribution (CC BY) license (<http://creativecommons.org/licenses/by/4.0/>).